EFFICIENCY OF TWO-WAVE MIXING VIA DYNAMIC BRAGG GRATINGS IN Er-DOPED OPTICAL FIBERS

S. STEPANOV, M. PLATA[1]

UDC 535.215

CICESE
(km.107 carr.Tijuana-Ensenada, Ensenada, 22860, México),

[1]**INAOE**
(Ap.post. 51 y 216, Puebla, 72000, México)

Efficiency of dynamic Bragg gratings recorded in Er-doped optical fibers via spatial hole burning in the configuration of two-wave mixing is evaluated. The analysis performed in the approximation of low grating contrast and undepleted recording waves takes into account a large-scale saturation of fiber optical absorption. Direct comparison with the experimental results obtained on transient and stationary two-wave mixing (TWM) in an Er-doped fiber at 1549 nm resulted in disagreement by a factor ≈7, which cannot be explained by the polarization mismatch of recording waves only.

Introduction

The effect of spatial hole burning is well known in the physics of lasers for decades [1]. In particular, in standing-wave lasers, it demonstrates itself as a local saturation of gain of the inverted media in maxima of the interference pattern, which is formed by two coherent waves traveling inside a laser cavity in the opposite directions. Spatial concentration of the dominant mode power inside these maxima prevents from a free intermode competition for the pump power, which usually results in the multi-frequency operation of these lasers.

In a recent publication [2], the utilization of spatial hole burning in Er-doped optical fibers for recording of dynamic Bragg gratings was proposed and experimentally demonstrated. Physical "thickness" (i.e. the fiber length L) of such reflectance gratings can be rather big: up to 12 m in the reported experiments [2]. For this reason, their spectral selectivity proves to be extremely high and such fiber gratings can be attractive candidates for the realization of tunable narrow-band (with the frequency band down to tens of MHz) optical filters [2–7].

Clearly, the spatial hole burning is possible not only in optically pumped laser media (which results in recording of dynamic gain grating), but in not pumped ones as well. As a result of the local saturation of optical absorption, the formation of amplitude gratings (i.e. of conventional absorption gratings) can also be observed in doped fibers. As was originally proposed and experimentally demonstrated in [8,9] (see also later publications [10,11]), the incorporation of a piece of a doped but not pumped fiber in a standing-wave fiber laser can result in essentially single-frequency operation. It is supposed that the amplitude dynamic grating, which is formed in this additional doped piece of the fiber, works as a highly selective intracavity saturable filter, which ensures the survival of the dominant laser mode only.

Even these two above-mentioned applications (i.e. tunable narrow-band filters and realization of single-frequency standing-wave lasers) justify detailed investigations of the dynamic Bragg gratings recorded in the rare-earth doped optical fibers. From our point of view, applications of such gratings in more traditional configurations of dynamic holography (e.g., for adaptive laser vibrometry, profilometry, fiber sensors, etc.), where bulk or film photosensitive materials are traditionally used, are also highly promising. Here, the possibility of sub-mW operation, easy light amplification, all-fiber realization of adaptive interferometers, and commercial availability of practically all necessary system elements are potentially very attractive. Commercially available multimode rare-earth doped fibers also open the way for the utilization of this technology for the processing of coherent images and for the optical phase conjugation.

The experimental data, published by the present moment on dynamic fiber gratings, are, however, not systematic, obtained for randomly selected fiber types, lengths, and recording laser powers and wavelengths. Note also that the majority of reported experiments was performed with Er-doped fibers (with the recording wavelengths from the 1520—1536 nm spectral region) with the only exception of Yb-doped fibers (at $\lambda = 1040$ nm) [11]. Detection of the recorded gratings is usually performed using the four-wave mixing configuration (in fact, pump-and-probe one) [2–5, 7] with rather different

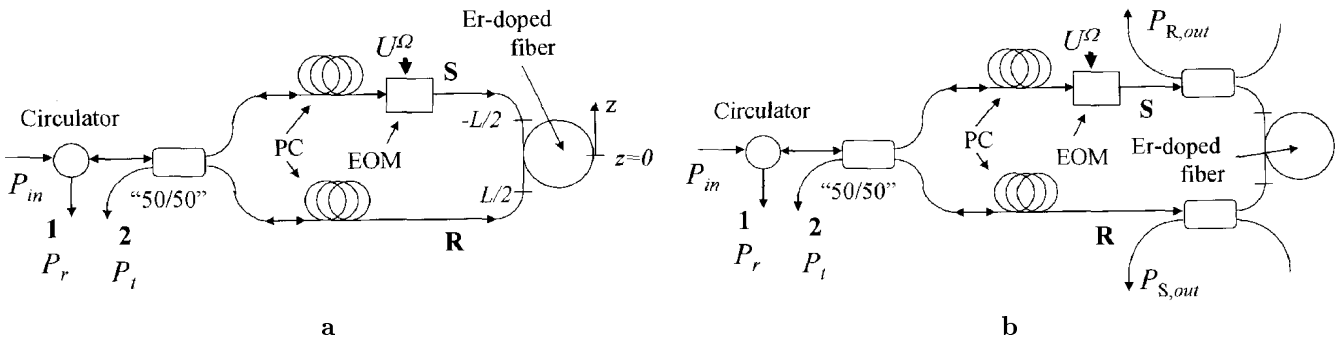

Fig. 1. *a* — schematic of a Sagnac interferometer used for the recording of dynamic reflectance Bragg gratings in Er-doped optical fibers (PC — polarization controllers, EOM — electro-optic phase modulator). *b* — modified Sagnac interferometer with two additional couplers which enable the separate detection of waves transmitted through the doped fiber with grating

estimations of the recorded grating efficiencies — from a quite high value of 75%, reported in [2] for 12 m long optically pumped fiber, to significantly lower values, which can be evaluated from experimental data presented in the above-mentioned later publications. As far as we know, any detailed theoretical analysis of the grating diffraction efficiency (and its comparison with the experimental data) is also absent. The Kramers—Kronig relations also permit the admixture of a phase component in the recorded grating [2,12], but, as far as we know, no experimental verification of this possibility was done.

The purpose of this paper is to present some simplified, rather heuristic theoretical evaluation of the grating efficiency as it is observed in the configuration of TWM, which is more typical of applications in dynamic/adaptive interferometry. The theoretical estimations obtained are compared with the results of original experiments on transient/stationary TWM in Er-doped fibers without optical pumping. In this comparison, the experimental data on the large-scale saturation of fiber optical absorption are used in essential way.

1. Theoretical Analysis of Grating Efficiency in the TWM Configuration

Below we consider some typical conditions of the dynamic grating recording without optical pumping of a fiber and the expected amplitude of a TWM signal. The analysis is performed in the approximations of low grating contrast and undepleted interacting waves. One of the main problems, which we address here, is the large-scale variations of fiber optical absorption induced by two counterpropagating beams participating in recording of the grating.

1.1. Recording Configuration

The basic configuration, which is usually considered in relation with recording of the dynamic fiber gratings, is a Sagnac interferometer — see Fig. 1,*a*. In this arrangement, two counterpropagating recording waves S and R (in the following, we generally consider the simplest case of their equal input powers) are derived from an initial input wave by means of an input 50/50 fiber coupler. We assume that the interferometer has the arms of equal length (as measured from the center of the doped fiber piece, located at $z = 0$ in Fig. 1,*a*) and the coherence length L_c of the laser source is bigger than the length of the doped piece of the fiber L. This is obviously the necessary (but not sufficient) condition for the formation of a high contrast interference pattern through the whole doped fiber length.

As well known, TWM configurations do not need any additional probe wave to observe the recorded grating — its presence is detected via stationary (in case of stationary TWM) or transient (for transient TWM) changes in the transmitted recording wave powers ($P_S(L/2)$ and $P_R(-L/2)$ in Fig. 1,*a*). Conventional arrangement of a Sagnac interferometer does not possess, however, the possibility to observe these two waves separately. To enable this, two additional couplers are to be incorporated in the set up — see Fig. 1,*b*. In turn, the Sagnac interferometer has two outputs: "1" where the so-called reflected power P_r goes to (it can easily be observed using a circulator located in front of the interferometer — Fig. 1,*a*) and "2" — for the transmitted

power P_t. In case of an ideal 50/50 input coupler without losses and the interferometer loop without birefringence both transmitted waves (S($L/2$) and R($-L/2$)) are constructively summarized at the main output "1" and interfere destructively at the other output "2" (see e.g. [13]). In this way, one can use terminal "1" of the Sagnac interferometer to observe the coherent sum of two transmitted waves.

Another problem typical of the experimental setups, which utilize conventional (not polarization preserving) single-mode fibers, is a spatially variable mismatch in polarizations of the counterpropagating recording waves due to a possible random birefringence of optical fibers (both doped and not doped) along the interferometer loop. In fact, the birefringence in the interferometer loop destroys the above-mentioned balance between the output powers (P_r and P_t) from the Sagnac interferometer. In particular, the incorporation of birefringence equivalent to a half-wavelength plate (with the fast axis oriented at $\pm 45°$ with respect to the configuration plane and to the initial input linear polarization of the light) redirects all the optical power into output "2" [13]. The polarizations of the counterpropagating beams prove to be essentially orthogonal through the interferometer length in this case. To restore the output powers balance (and to maximize an average contrast of the interference pattern), polarization controllers are usually adjusted to minimize the output from terminal "2".

For simplicity, we neglect the above-mentioned possible fiber birefringence and assume that optical elements forming the closed loop of the interferometry do not introduce optical losses. Obviously, we cannot do the latter for an Er-doped fiber: the local saturation of optical absorption of this fiber gives rise to the dynamic grating under consideration. For this reason, we have to include in our analysis the attenuation of recording waves through the doped fiber length, i.e. to consider their powers as coordinate-dependent: $P_S(z)$ and $P_R(z)$.

1.2. Grating Amplitude

For any particular short piece of a doped fiber, we can assume, however, that powers of these two recording waves are fixed and consider that the grating recording is ensured by some sinusoidal interference pattern:

$$P(z) = P_0 \left[1 + m \cos\left(Kz\right)\right]. \tag{1}$$

Here, P_0 is the average total light power, m is the recording pattern contrast, and $K = 2\pi n/\lambda$ is the grating spatial frequency (n is the effective refractive index of the fiber and λ is the recording wavelength). Note that while K is constant, both P_0 and m can vary through the fiber length, but significantly slower than the periodic light power variations in the interference pattern.

In consideration of the grating formation, we use a simple relation (see e.g. [3,4,12,14]) which describes the saturation of the initial optical absorption of a fiber α_0 under the local value of the light power $P(z)$:

$$\alpha(z) = \frac{\alpha_0}{1 + P(z)/P_{\rm sat}}. \tag{2}$$

Here, the so-called "saturation power" $P_{\rm sat}$ is some characteristic parameter of the dopant (which depends on the cross-section of the optical absorption and life-time of the excited state) and also of the fiber itself (i.e. on the core diameter, mode, and dopant distribution through the fiber cross-section). Dependence of the final, i.e. saturated, optical absorption on P is clearly essentially nonlinear. In approximation of low contrast of the recording light pattern ($m \ll 1$), it can be linearized with respect to m by the following relation:

$$\alpha(z) = \frac{\alpha_0}{1 + P_0/P_{\rm sat}} - m\alpha_0 \frac{P_0/P_{\rm sat}}{(1 + P_0/P_{\rm sat})^2} \cos(Kz) =$$

$$= \alpha \left[1 + m_g \cos(Kz)\right]. \tag{3}$$

The first term on the right-hand side of the above equation gives us the average level of the saturated optical absorption α, while the second term — the recorded grating amplitude. Note that the absolute value of the grating amplitude reaches its maximum for $P_0 = P_{\rm sat}$, while the modulation depth, i.e. the contrast of the grating,

$$m_g = -m \frac{P_0/P_{\rm sat}}{1 + P_0/P_{\rm sat}}, \tag{4}$$

keeps always growing with the $P_0/P_{\rm sat}$ ratio. Negative sign on the right-hand side of the above equation corresponds to the typical feature of the amplitude gratings recorded via spatial hole burning: the minima in the absorption profile are located in the maxima of the light pattern — Fig. 2,*a*.

Numerical simulation (Fig. 2,*b*) shows that Eq. (4) obtained for m_g in the approximation of low contrast of the recording pattern is incorrect for relatively high values of m approaching 0.9—1 only, when m_g demonstrates some additional growth. For this reason, we can use Eq. (4) in the following evaluations of the TWM efficiency "from below". Note that the saturation of average optical absorption α also demonstrates some reduction at a high pattern contrast — see Fig. 2,*c*.

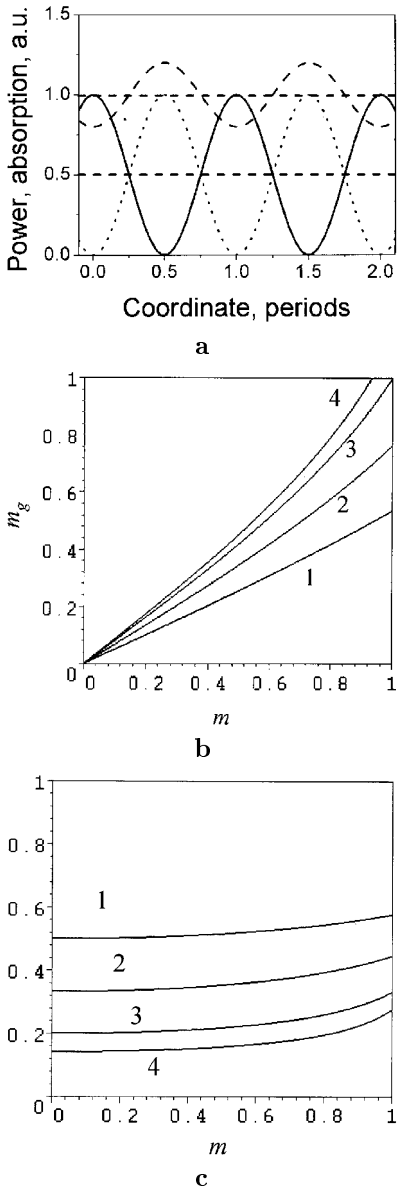

Fig. 2. *a* — diagram illustrating the phasing of the light power profile (solid line) and absorption profile (average level and fundamental Bragg component are shown by dashed lines only) in steady-state case. Dotted line shows the light power distribution in the interference pattern shifted by half of the spatial period (i.e. when $\pm\pi$ phase shift is introduced in one of the recording waves). *b* — effective Bragg grating contrast m_g (i.e. relative value of the first, fundamental spatial component in the grating profile) as a function of m, as calculated from Eqs.(1) and (2) for different $P_0/P_{\rm sat}$ ratios: *1* — 1, *2* — 2, *4* — 3, and *6* — 4. *c* — reduction in the average absorption coefficient of the grating as a function of m, as calculated from Eqs. (1), (2) for different $P_0/P_{\rm sat}$ ratios: *1* — 1, *2* — 2, *4* — 3, and *6* — 4

1.3. Large-scale Saturation of Fiber Absorption

The characteristic feature of the doped fibers under consideration is a significant saturation of their optical absorption (Eq. (2)) with light powers of sub-mW level. This ensures the amplitude grating recording, but, on the other hand, changes dramatically light propagation even in case of one wave, or for two counterpropagating waves without grating formation (e.g. for mutually incoherent waves). In particular, in case of one wave only (for example, the signal one) the equation which describes the light power propagation with the saturation of absorption is the following one:

$$\frac{\partial P_S}{\partial z} = -\alpha P_S = -\frac{\alpha_0 P_S}{1 + P_S/P_{\rm sat}}. \tag{5}$$

This nonlinear differential equation can be solved analytically, which gives us the following type of light attenuation after the propagation through the fiber length L:

$$\frac{P_{S,\rm out}}{P_{\rm sat}} = W\left[\frac{P_{S,\rm in}}{P_{\rm sat}}\exp\left(\frac{P_{S,\rm in}}{P_{\rm sat}} - \alpha_0 L\right)\right]. \tag{6}$$

Here, $P_{S,\rm in}$ and $P_{S,\rm out}$ are the input and output light powers, respectively, and W is the Lambert's W function (i.e. the solution of the equation $W(x)\exp(W(x)) = x$).

Dependence of the normalized output power $P_{S,\rm out}/P_{\rm sat}$ on the normalized input power $P_{S,\rm in}/P_{\rm sat}$ calculated using Eq. (6) for different values of the initial fiber optical densities is given in Fig. 3,*a* with corresponding linear approximations obtained for high input powers. Simplifying, one can say from here that the first $\alpha_0 L$ part of the normalized input power $P_{S,\rm in}/P_{\rm sat}$ is basically used for the saturation of fiber absorption, while the rest propagates practically without attenuation.

The same simple rule is valid for the more complicated case of two mutually incoherent waves of equal input powers ($P_{S,\rm in} = P_{R,\rm in} = P_{\rm in}/2$) counterpropagating through the fiber. If the total normalized input power $P_{\rm in}/P_{\rm sat}$ exceeds the initial optical density $\alpha_0 L$, the optical absorption is saturated in an essential way. The equations for the light power propagation

$$\frac{\partial P_S}{\partial z} = -\frac{\alpha_0 P_S}{1 + P_S/P_{\rm sat} + P_R/P_{\rm sat}};$$

$$\frac{\partial P_R}{\partial z} = \frac{\alpha_0 P_R}{1 + P_S/P_{\rm sat} + P_R/P_{\rm sat}} \tag{7}$$

and their analytical solution, which can also be obtained in terms of Lambert's W functions, are more complicated

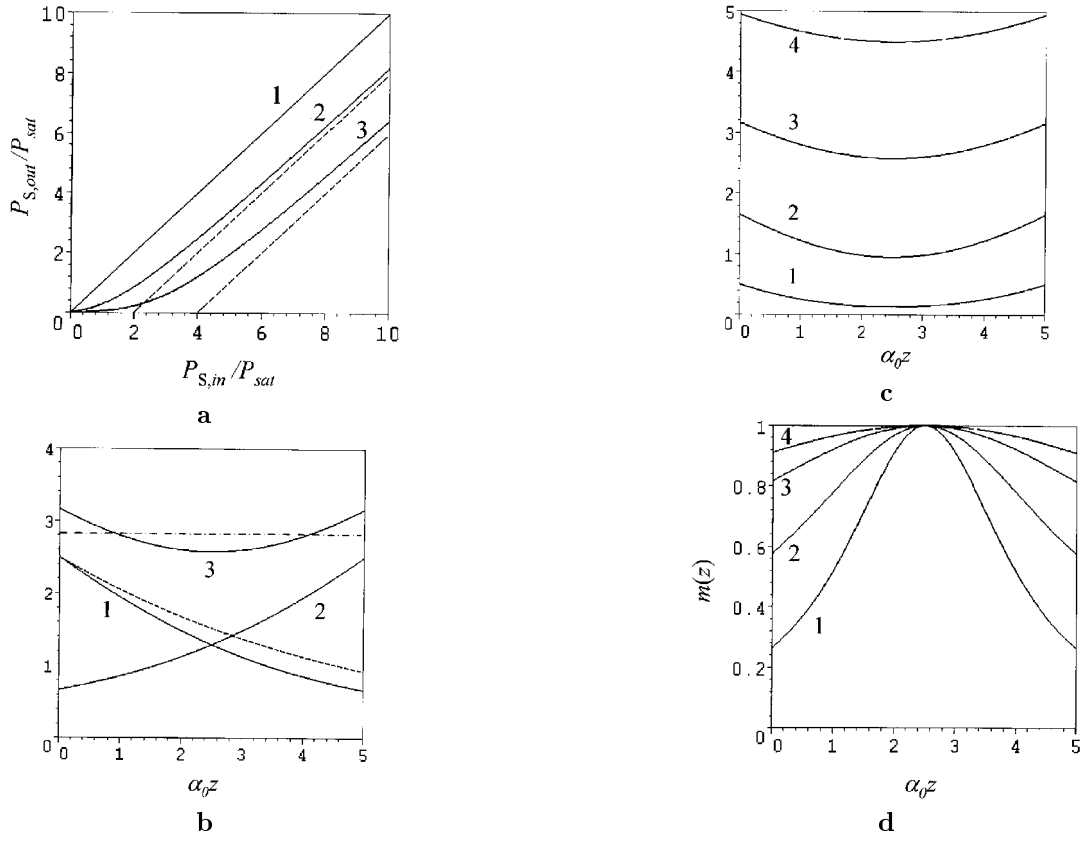

Fig. 3. *a* — normalized output power ($P_{S,\mathrm{out}}/P_{\mathrm{sat}}$) versus normalized input power ($P_{S,\mathrm{in}}/P_{\mathrm{sat}}$) as calculated from Eq. (6) for different initial densities of a doped fiber $\alpha_0 L$: *0* — 1, *2* — 2, *4* — 3 (one incident wave S only). Dashed lines present the corresponding linear approximations for high input powers. *b* — normalized spatial power profiles of two counterpropagating waves (*1* and *2*) and of their incoherent sum (*3*) obtained for symmetric illumination ($P_{S,\mathrm{in}} = P_{R,\mathrm{in}} = P_{\mathrm{in}}/2$) of the saturated optical fiber with initial optical density $\alpha_0 L = 5$ with total normalized input power $P_{\mathrm{in}}/P_{\mathrm{sat}} = 5$. Dashed line shows the conventional (exponential) attenuation of one of the waves through a fiber with optical density $\alpha L = 1$. *c* — spatial profiles of total normalized power, obtained for symmetric illumination ($P_{S,\mathrm{in}} = P_{R,\mathrm{in}} = P_{\mathrm{in}}/2$) of the optical fiber with initial optical density $\alpha_0 L = 5$ with total normalized input power $P_{\mathrm{in}}/P_{\mathrm{sat}}$: *1* — 1, *3* — 2, *5* — 3, *7* — 4. *d* — spatial profiles of the interference pattern contrast $m(z)$ observed under similar (as in Fig. 3,*c*) conditions

in this case. As an illustration, Fig. 3,*b* presents a set of power profiles for two separate waves ($P_S(z)/P_{\mathrm{sat}}$, $P_R(z)/P_{\mathrm{sat}}$) and for their sum ($[P_S(z) + P_R(z)]/P_{\mathrm{sat}}$) for the typical case of $\alpha_0 L = 5$ and $P_{\mathrm{in}}/P_{\mathrm{sat}} = 5$. One can see that, in this case, the initial optical density of the fiber is reduced significantly to the value close to 1. The distribution of total light power proves to be very close to the uniform one (Fig.3,*b,c*) with an average level $\approx 2.8 P_{\mathrm{sat}}$. The contrast of the interference pattern, which these two waves can form in case of their complete mutual coherence, varies from the maximum value 1 at the center of the doped fiber to the minimum value $\approx$ ≈ 0.8 near the ends — Fig. 3,*d*.

Detailed numerical simulation supports the same general result: if the fiber with an initial optical density $\alpha_0 L$ is illuminated from both sides by two counterpropagating beams with the total input power $P_{\mathrm{in}}/P_{\mathrm{sat}} \approx \alpha_0 L$ equally distributed between two inputs, the initial optical density of the fiber is reduced approximately to ≈ 1. Also, the contrast of the interference pattern through the fiber differs from the maximum value $m = 1$ insignificantly only. This allows us to use the rather simple approximation of constant optical absorption coefficient and modulation depth of the amplitude grating (which are observed in a special case of $P_{\mathrm{in}}/P_{\mathrm{sat}} \approx \alpha_0 L$) in the following analysis of the

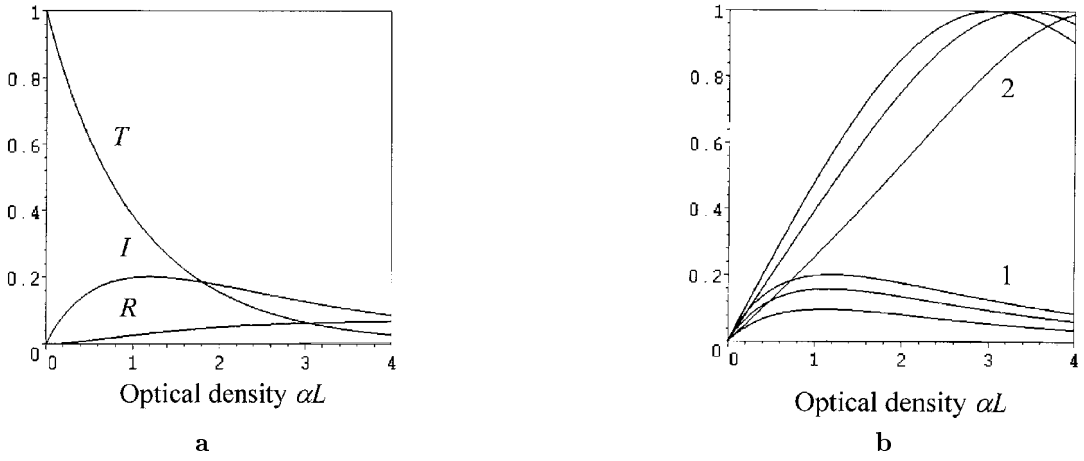

Fig. 4. *a* — transmittivity T, reflectivity R, and interference term $I = 2\sqrt{TR}$ for the amplitude grating with absorption as functions of the grating optical density αL ($m_g = 1$). *b* — absolute (*1*) and normalized to $(T + R)$ (*2*) values of the interference term I as functions of grating optical density αL for different grating contrasts m_g: 1, 0.8, 0.5 (from the top to the bottom)

grating recording. Note that the utilization of lower input powers changes the profiles of total light power and interference pattern contrast dramatically — see Fig. 3,*c*,*d*.

1.4. Light Self-diffraction from the Recorded Amplitude Grating

In the following consideration of self-diffraction of the recording waves (i.e. of TWM,) we use the conventional system of coupled wave equations [15] in their simplest form with exact satisfaction of the Bragg conditions:

$$\frac{\partial \mathrm{S}}{\partial z} = -\frac{\alpha}{2}\left(\mathrm{S} + \frac{m_g}{2}\mathrm{R}\right),$$

$$\frac{\partial \mathrm{R}}{\partial z} = \frac{\alpha}{2}\left(\mathrm{R} + \frac{m_g}{2}\mathrm{S}\right). \qquad (8)$$

Here, S and R are the slowly varying amplitudes of counterpropagating waves (i.e. their complex amplitudes without rapidly oscillating factors $\exp(-iKz)$ and $\exp(iKz)$, respectively). The sinusoidal amplitude grating has the presented above form (Eq. (3)), and both the average optical absorption α and the grating contrast m_g are supposed to be constant through the fiber length in this obviously simplified analysis.

Fig. 4,*a* presents the powers of the transmitted ($T = |\mathrm{S}(L/2)|^2$) and reflected ($R = |\mathrm{R}(-L/2)|^2$) waves, when one wave (namely S) with unit input amplitude is incident into the grating only: $\mathrm{S}(-L/2) = 1$; $\mathrm{R}(L/2) = 0$. T (transmittivity) and R (reflectivity) are plotted as functions of optical density of the fiber αL for a model case of maximum grating contrast $m_g = 1$. Because of a complete symmetry of configuration, T and R will be the same for incidence from the opposite side of the grating ($\mathrm{S}(-L/2) = 0$; $\mathrm{R}(L/2) = 1$). For this reason, when two counterpropagating waves with equal unit input amplitudes ($\mathrm{S}(-L/2)$=1; $\mathrm{R}(L/2)$=1) are incident simultaneously, we have two waves propagating away from the grating at every of two opposite ends of the fiber: one wave with the power equal to T (i.e. transmitted wave) and another one with the power equal to R (i.e. reflected from the grating wave). While, in the pump-and-probe experiment, we are interested in the power of a reflected wave (i.e. in the diffraction efficiency of the grating equal to R in our consideration), in the TWM experiment, we usually measure a more powerful interference (constructive or destructive) between these two waves with the power $I = 2\sqrt{TR}$. This interference term I is also presented in Fig. 4,*a* and, as follows from this curve, it reaches its absolute maximum at $\alpha L \approx 1$ (or to be more exact at $\alpha L = \ln 3 \approx 1.1$ in the approximation of low m_g).

The above-mentioned optimal condition (i.e. $\alpha L \approx 1$), which maximizes the absolute value of the TWM signal, practically does not depend on the grating contrast — see Fig. 4,*b*. In the experiment, it is usually more convenient to measure the relative value of this signal normalized to the total average light power leaving the fiber, i.e. to the incoherently summarized transmitted and reflected powers: $\gamma = I/(T+R)$. As one can also see from Fig. 4,*b*, the position of a maximum in

the $\gamma(\alpha L)$ curve is, however, essentially m_g dependent. For this reason, in practice, the selection of the right parameter (I or γ) to optimize the TWM configuration depends on every particular application (for example, on dominant noise of the photodetector). For purposes of the present analysis, we assume the condition $\alpha L \approx 1$ (maximizing the absolute value of the interference term) as the optimal one. As a result, in the approximation of a small grating contrast ($m_g << 1$), two parameters characterizing the efficiency of TWM have the following values:

$$I \approx 0.19 m_g,$$

$$\gamma = m_g \sinh\left(\frac{\alpha L}{2}\right) \approx m_g \frac{\alpha L}{2}. \tag{9}$$

1.5. Evaluation of TWM Signal Amplitude

As one can see, TWM via dynamic Bragg gratings in doped fibers includes at least three important aspects: nonlinear wave propagation through the fiber with a large-scale saturation of optical absorption, grating formation through local saturation of absorption in maxima of the interference pattern, and diffraction of the recording beams from the recorded grating. All these three parts of the process are essentially nonlinear and mutually connected to each other. For complexity of this problem it is not clear whether it is possible to develop any theoretical analytical approach. Of course, a numerical simulation is always possible and should be done. However, as follows from the above consideration of these different aspects, some simplified analytical approach to the evaluation of the TWM efficiency is possible for the recording conditions, which are very close to the optimal.

It can be based on the approximation of low contrast of the recording pattern (and that of the recorded grating), which, as was demonstrated above, is correct with a reasonably high accuracy up to the maximal values $m, m_g = 1$. Another important point is the fact that for total input power of the recording beams $P_{\text{in}}/P_{\text{sat}} \approx \alpha_0 L$, the initial optical density of the fiber $\alpha_0 L$ is saturated down to a relatively low value $\alpha L \approx 1$. This, in turn, ensures practically a uniform distribution of total light power ($P_0 = P_S + P_R$) and of the average contrast of the recording interference pattern m_a, approaching 1 through the whole fiber length. Note that this approximation is valid for the practically important case of the initial optical density $\alpha_0 L$ significantly exceeding 1 as well.

For this case we can evaluate the modulation depth of an amplitude grating by the value

$$m_g \approx -m_a \frac{P_0/P_{\text{sat}}}{1 + P_0/P_{\text{sat}}}. \tag{10}$$

Taking into account the saturated value of the fiber density $\alpha L \approx 1$, we can also use the value γ (Eq. (9)) for this particular case. All this gives:

$$\gamma \approx \frac{|m_g|}{2} \approx \frac{m_a}{2} \frac{P_0/P_{\text{sat}}}{1 + P_0/P_{\text{sat}}}. \tag{11}$$

Note also that the value $\alpha L \approx 1$ expected in this case corresponds to the optimal one which maximizes the absolute value of the TWM signal.

2. Experimental Results

Below, we present the experimental results on transient TWM, which were obtained for single-mode Er-doped optical fiber EDF-HG980. In accordance with the data sheet of the supplier (OFS-Fitel), this is a rather heavily doped fiber with maximal absorption about 8—14 db/m at $\lambda = 1530$ nm. In the reported experiments, we used a 3 m long piece of this fiber spliced between two pieces of a conventional (not doped) single-mode fiber terminated with standard FC connectors.

In general, our experimental setup copied the schematic diagram presented above in Fig. 1,*a*. Note that all optical elements of the configuration were connected via FC connectors immersed with glycerine. In one arm of the Sagnac interferometer, an electro-optic modulator was additionally incorporated, which was used to introduce the step-like phase modulation in one of the recording waves. As a source of coherent radiation, we used a pig-tailed DFB InGaAsP semiconductor laser with 2 mW output at $\lambda = 1549$ nm. Special measurements confirmed that, under the optimal operation temperature, the laser coherence length was big enough ($L_c > 10$ m) to ensure a high visibility of the interference pattern through the whole length ($L = 3$m) of the doped fiber. Input power P_{in} was changed in our experiments by an additional variable attenuator placed in front of the circulator in Fig. 1,*a*.

The measurement of optical absorption of a doped fiber prepared in the above-mentioned way in the spectral range 1400—1650 nm (broader than the typical absorption line of Er^{3+} — see the inset in Fig. 5) showed that splices between doped and non-doped fibers introduced additional light power losses about 20% for one splice. Initial optical density of the doped fiber at

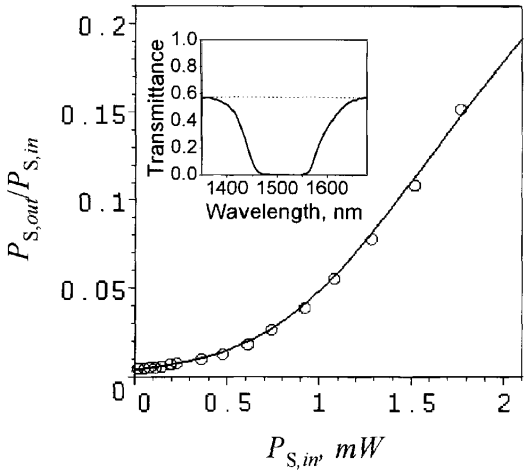

Fig. 5. Transmittance ($P_{S,\mathrm{out}}/P_{S,\mathrm{in}}$) of the fiber as a function of input power $P_{S,\mathrm{in}}$ (Er-doped fiber HG980, $\alpha = 1549$ nm). Solid line shows the theoretical approximation curve calculated from Eq. (6) using the fitting parameter $P_{\mathrm{sat}} = 0.30$ mW and taking into account the light power losses $\approx 40\%$ for two splices. Inset shows the transmittance curve obtained using an internal incoherent light source of the spectrophotometer

the laser wavelength was $\alpha_0 L \approx 5$. Fig. 5 presents the dependence of transmittance ($P_{S,\mathrm{out}}/P_{S,\mathrm{in}}$) of the doped fiber as a function of the incident power $P_{S,\mathrm{in}}$ obtained for one incident beam only. Solid line in Fig. 5 corresponds to the theoretical curve derived from Eq. (6) taking into account the above-mentioned light losses at splices. The only fitting parameter used was the fiber saturation power $P_{\mathrm{sat}} \approx 0.30$ mW. In accordance with our theoretical analysis for this P_{sat}, the maximal output power of the DFB laser used was very close to the value (i.e. $P_{\mathrm{in}} \approx \alpha_0 L P_{\mathrm{sat}}$) which is needed to saturate our fiber significantly.

Fig. 6,*a* shows a typical oscilloscope trace which was obtained, when the periodic rectangular phase modulation with a peak-to-peak amplitude of π was introduced via an EO modulator. In this experiment, one of the polarization controllers, namely that located in front of the EO modulator, was adjusted to ensure the vertical linear input polarization optimal for this device. By adjusting another polarization controller, we maximized the output transient TWM signal, which was also accompanied by minimization of the average level of the light power transmitted through the Sagnac interferometer (i.e. that detected at output "2" — see Fig. 1,*a*). To obtain these oscilloscope traces, we used the averaging regime of a digital oscilloscope. It was done to reduce the slowly fluctuating output signal with a rectangular profile of the modulation signal. As we believe, it appeared as a result of interference due to residual reflections from the connectors inside the interferometer and randomly fluctuated with the environmental temperature.

The relative (i.e. divided by a dc signal level) amplitude of the detected transient signal first demonstrated some growth with the input power, which was followed by saturation at the maximal available laser output power (Fig. 6,*b*). As to the modulation amplitude, the signal, as expected, reached its maximal value for $\approx \pi$ peak-to-peak amplitude of phase modulation reached in our EO modulator at $\approx 2V_{p-p}$ of the driving voltage (see the inset in Fig. 6,*b*).

The negative transient peaks (Fig. 6,*a*) appearing in the reply to every step-like phase change (i.e. both for positive and negative phase jumps) result from the spatial shift of the recording interference pattern by half of the spatial period $\Lambda/2$, which instantly changes the constructive interference between the beams transmitted through and reflected from the dynamic amplitude grating for destructive one. From the diagram presented in Fig. 2,*a*, one can see that, after such a fast displacement, the maxima of the interference pattern overlap with the maxima of absorption in the recorded grating. This changes the grating-induced reduction in the recording waves absorption for similar increase in their absorption. After this, the grating returns to a new position of the interference pattern (which restores the initial level of the reduced absorption) with the characteristic time of the grating formation τ_g.

The relative amplitude of the peaks observed in Fig. 6,*a* ($\approx 8\%$) approximately corresponds to the duplicated value of the stationary TWM signal observed in the configuration of Fig. 1,*a*, but without EO modulator. In this case, we measured the difference between the light powers reflected from the Sagnac interferometer in cases of the recording light of high coherence (i.e. when the dynamic grating is formed) and of low coherence (without grating formation). The latter regime of low coherence (with L_c of some millimeters) was realized by a simple change of the DFB laser driving current (or operation temperature) from its optimal value. For the maximal output laser power available, the reflectivity of the configuration was $\approx 4.5\%$ bigger in case of coherent light, i.e. we observed the grating-induced growth in the transmittance of the fiber. A small deviation of the value observed from a half of that obtained from the transient TWM (i.e. $\approx 4\%$) can be explained by a somewhat reduced average level of the light power and the contrast of the recording pattern in the latter experiment. It was

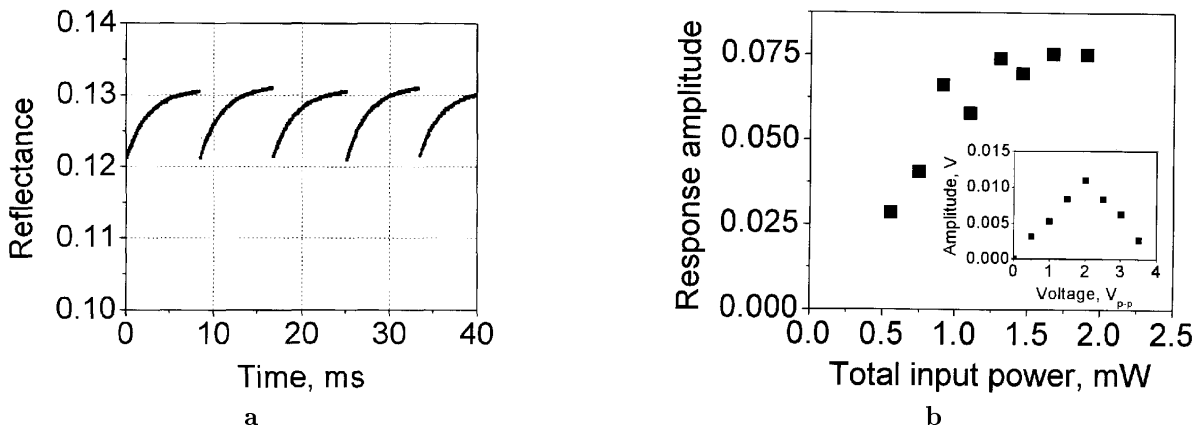

a b

Fig. 6. *a* — oscilloscope trace of the transient TWM signal in response to rectangular phase modulation with peak-to-peak amplitude π and modulation frequency 60 Hz. *b* — relative amplitude of the transient TWM signal amplitude as a function of total input power. Inset shows dependence of the signal amplitude on driving voltage applied to EO modulator

due to a relatively low transmission ($\approx 30\%$) of the EO modulator used.

We also performed the experiments on transient TWM with sinusoidal phase modulation. As could be expected from the response to the rectangular modulation (Fig. 6,*a*) in this case, we managed to detect a stable output signal at the second harmonic (2Ω) of the modulation frequency Ω only. For this type of modulation, we also measured partial output signals in the light beams transmitted through the doped fiber in the opposite directions using two additional couplers, as shown in Fig. 1,*b*. No significant admixture of a stable output at the fundamental harmonic of the modulation frequency was observed. In turn, the partial output signals detected at the second harmonic proved to be in phase. This result rules out the possibility of any significant admixture of a phase component in the grating, for which the energy exchange can be observed.

We performed the same experiments with other Er-doped fibers as well. In particular, similar results (in respect with the TWM signal amplitude and the shape of transient response) were also observed for an OFS-Fitel EDF-555 fiber ($L = 3$ m with $\alpha_0 \approx 8.7$ db/m at 1530nm) and for a High-Wave Optical Technologies Er-doped fiber ($L = 5$ m with $\alpha_0 \approx 4$ db/m at 1532 nm).

3. Discussion

The results obtained in our transient TWM experiments indicate that we observe the unshifted amplitude dynamic gratings, with minima of absorption located in maxima of the recording interference pattern. Indeed, the doped fiber as a medium for the recording of dynamic gratings has no preferred direction. For this reason, if we neglect an asymmetry introduced externally (as, e.g., a possible difference in the input powers of counterpropagating waves), there is no reason for the recorded grating to be a shifted one. In turn, the presence of the significant phase component is ruled out by the absence of fundamental harmonic components in the output powers of the waves transmitted through the fiber into opposite directions (the periodic energy exchange between these two waves cannot be detected in the total power reflected from the Sagnac interferometer). The above-mentioned location of the amplitude grating minima is supported, in particular, by the sign of transient signals observed in Fig. 6,*a*: any displacement of the interference pattern from the steady-state position results in a growth of the light absorption. All these facts correspond to the amplitude grating recorded via spatial hole burning (i.e. by the local saturation of fiber optical absorption).

As we mentioned above, for the numerical evaluation of the TWM amplitude, we can use the simplified approach developed above. Indeed, the fiber in the experiments has the initial optical density $\alpha_0 L \approx 5$, $P_{\rm sat} \approx 0.30$ mW, and the maximal input power which enters the doped part of the fiber is ≈ 1.6 mW, i.e. $P_{\rm in}/P_{\rm sat} \gtrsim \alpha_0 L$. The numerical simulation (see Fig. 3,*b*,*d*) shows that, for this combination of parameters, the average power inside the fiber is around $\approx 2.8 P_{\rm sat}$ and the average interference pattern contrast $m \approx 0.9$. Substituting these values into Eq. (11), one can evaluate the expected value of γ as $\gtrsim 0.3$. In turn, the maximal

value $\gamma_{\exp}$ obtained from our transient/stationary TWM experiments was around $(4 \div 4.5) \cdot 10^{-2}$: i.e. we indeed observe a significant (by a factor ≈ 7) disagreement between the experimentally observed efficiency of TWM and its theoretical estimation. Note also that the experimentally observed TWM amplitude allows us to evaluate the diffraction efficiency of the recorded amplitude grating as $\eta \approx \exp(-\alpha L) * (\gamma_{\exp}/2)^2 \approx 10^{-4}$.

One of the possible reasons for this discrepancy can be the mismatch between polarizations of the recording waves counterpropagating through the fiber. It is basically because of random birefringence of the doped fiber due to defects of fabrication, mechanical stress, and coiling of the fiber. If this is present, it can reduce the effective contrast of the recording interference pattern, reducing in this way the observed TWM amplitude. However, this reason can hardly explain the disagreement mentioned above: for example, in case of a very strong randomly distributed birefringence, it is reasonable to assume that, through a half of the fiber length, the waves have similar polarization, while through another half — the orthogonal one. This can, however, reduce the efficiency of TWM by a factor of two only. Note also that this reason can be verified experimentally or may even be eliminated completely by using a doped fiber which supports polarization or by introducing a significant regular birefringence by coiling the fiber around some cylinder of a small radius.

Another, more fundamental reason (proposed earlier in [5]) can be due to a resonant migration of the excited state between neighboring Er^{3+} ions. Indeed, the commercially available Er-doped fibers, which we use in our experiments, were developed for applications in optical fiber amplifiers or lasers. A general trend in the development of effective Er-doped fibers for these purposes is to increase the dopant concentration maximally. This, however, reduces the inter-ion distances and enables the effective interaction between neighboring Er^{3+} ions. There are different effects associated with such nonradiative interactions (e.g., fluorescence self-quenching and cooperative frequency upconversion) which, beginning from some certain dopant concentration, result in diminishing fluorescence and light amplification (see, e.g., [16]).

The effects mentioned above use the additional (higher) energy levels of Er^{3+} in an essential way. There is, however, another simpler type of the interaction between the neighboring Er^{3+}, which involves two low-energy levels only (namely $^4I_{15/2}$ and $^4I_{13/2}$ which give rise to fundamental optical absorption and light amplification at $\lambda \approx 1.5\mu$m in Er-doped glasses). This is the effect of resonant energy migration [16], when one ion in the excited state transfers its excitation to the neighboring ion via a nonradiative process and returns to the ground state. In turn, the second ion can also transfer its excitation to another ion, etc., resulting in this way in a random walk of the excitation energy through the bulk of material.

Because of its random nature, this migration process reduces the contrast of the spatial distribution of excited Er^{3+} ions (i.e. the contrast of the recorded amplitude grating) as compared with the initial contrast of the recording interference pattern. It is supposed [16] that the physical mechanism of this nonradiative energy exchange is the multipole interaction between Er^{3+} ions, which depends on the average distance between them (i.e. on the dopant concentration) quite strongly. Note that this process of excitation migration does not influence the efficiency of average fluorescence or induced emission, and, for this reason, proves to be out of the scope of general investigations in optical fiber amplifiers.

For the Bragg gratings of the reflectance type under consideration, there is practically no possibility to change the grating spatial period significantly. For this reason, to verify a possible contribution of this effect to the formation of the dynamic grating, one has to perform experiments with a set of similar fibers differing by a level of doping only. Let us mention, however, one fact observed in our experiments, which probably indicates that this mechanism is really present. The characteristic decay time of the observed transient peaks (Fig. 6,*a*) was around 3 ms in this particular fiber, and, in accordance with the considered model, this is the characteristic formation time of the dynamic grating τ_g. In turn, in a simplest model of the grating formation via spatial hole burning which does not take into account the resonant excitation migration, the grating formation time is to be equal to the life-time of the Er^{3+} excited state $\tau \approx 9.5 \div 10.0$ ms in Al—Ge silica [17]. The grating life-time, as measured in our experiments, proves to be approximately three times shorter than the excitation state life-time for Er^{3+}. This clearly needs a more detailed verification, but this difference in combination with the above-mentioned possible effect of the polarization mismatch can roughly explain

the experimentally observed reduction in the grating amplitude.

Conclusion

In conclusion, we have investigated the efficiency of the two-wave mixing via dynamic Bragg gratings recorded in an Er-doped fiber via spatial hole burning. In particular, we developed a simple method for the evaluation of TWM efficiency for the practically important case of normalized (to the fiber saturation power) total input light power close to the initial optical density of the fiber. The experimental data on transient/stationary TWM obtained under similar conditions for a commercially available Er-doped HG980 fiber at $\lambda = 1549$ nm demonstrated the ≈ 7 fold reduction in the detected grating amplitude as compared with the expected value. The reduced TWM efficiency was also accompanied by the grating formation time approximately 3 times shorter than the characteristic life-time of the excited state of Er^{3+}. As the most probable reasons of the observed discrepancy, the polarization mismatch between the recording waves due to random fiber birefringence and the effect of resonant energy migration were discussed.

This work was performed in a partial fulfillment of CONACyT (Mexico) Project G25530A. Both authors like to express their gratitude to Dr. E.Kuzin from INAOE for the stimulating discussions and for the valuable technical assistance during the initial period of this work.

Using this pleasant opportunity and with kind permission of his co-author, S.Stepanov also expresses his deepest respect to Professor Marat Samoilovich Soskin as a Physicist and a Teacher and also all the best wishes for his future fruitful personal and professional life.

1. *Siegman A.E.* Lasers. — Sausalito: University Science Books, 1986.
2. *Frisken S.*//Opt. Lett. — 1992. — **17**. — P. 1776—1778.
3. *Fischer B., Zyskind J.L., Sulhoff J.W., DiGiovanni D.J.*// Electron. Lett. — 1993. — **29**. — P. 1858—1859.
4. *Fischer B., Zyskind J.L., Sulhoff J.W., DiGiovanni D.J.*// Opt. Lett. — 1993. — 18. — P. 2108—-2110.
5. *Feuer M.D.*// IEEE Phot. Tech. Lett. — 1998. — **10**. — P. 1587—1589.
6. *Kishi N., Yazaki T.*//Ibid. — 1999. — **11**. — P. 182—184.
7. *Havstad S.A., Fischer B., Willner A.E., Wickham M.G.* //Opt. Lett. — 1999. — **24**. — P. 1466—1468.
8. *Horowitz M., Daisy R., Fischer B., Zyskind J.* // Electron. Lett. — 1994. — **30**. — P. 648—649.
9. *Horowitz M., Daisy R., Fischer B., Zyskind J.L.* // Opt. Lett. — 1994. — **19**. — P. 1406—1408.
10. *Cheng Y., Kringlebotn J.T., Loh W.H. et al.* //Ibid. — 1995. — **20**. — P. 875—877.
11. *Paschotta R., Nilsson J., Reekie L. et al.*// Ibid. — 1997. — **22**. — P. 41—43.
12. *Desurvire E.*// J. Lightwave Technol. — 1990. — **8**. — P. 1517—1527.
13. *Mortimore D.B.*// Ibid. — 1988. — **6**.– P. 1217–1224.
14. *Agrawal G.P., Lax M.*// J. Opt. Soc. Amer. — 1981. — **71**. — P. 515—525.
15. *Kogelnik H.*// Bell System Techn. J. — 1969. — **48**. — P. 2909—2947.
16. *Desurvire E.* Erbium-doped Fiber Amplifiers. Principles and Applications. — New York: Wiley, 1994.
17. *Becker P.C., Ollson N.A., Simpson J.R.* Erbium-doped Fiber Amplifiers. Fundamentals and Technology. — San Diego: Academic, 1999.

ЕФЕКТИВНІСТЬ ДВОХВИЛЬОВОЇ ВЗАЄМОДІЇ ЧЕРЕЗ ДИНАМІЧНІ БРЕГГІВСЬКІ ГРАТКИ В ОПТИЧНОМУ ВОЛОКНІ З ДОМІШКОЮ ЕРБІЮ

С. Степанов, М. Плата

Р е з ю м е

Розраховано ефективність динамічної бреггівської гратки, записаної методом вигорання дірки в двопроменевій схемі в оптичних волокнах легованих ербієм. Аналіз проведено в наближенні низького контрасту гратки і невиснажених записуючих променів, враховуючи велике значення насичення оптичного поглинання в світловоді. Пряме порівняння з експериментальними даними, отриманими в перехідному і стаціонарному режимах двопроменевої взаємодії в оптичному волокні, легованому ербієм, на довжині хвилі 1549 нм, виявило розбіжність приблизно у 7 разів. Така розбіжність не може бути пояснена лише відмінністю у поляризації записуючих променів.